Journal of Cultural Heritage 71 (2025) 184–196

Contents lists available at ScienceDirect

Journal of Cultural Heritage

journal homepage: www.elsevier.com/locate/culher

Original article

Artificial induction of the “vinegar syndrome” in cellulose acetate motion picture film and multi-analytical protocol for its monitoring

Francesca Porpora[a], Luigi Dei[a], Alessia Maria Maiano[a], Emiliano Carretti[a,b,*]

[a] Department of Chemistry “Ugo Schiff” & CSGI Consortium, University of Florence – via della Lastruccia, 3-13 - 50019 Sesto Fiorentino FI, Italy
[b] CNR-INO, Largo E. Fermi 6, 50125 Florence FI, Italy

ARTICLE INFO

Article history:
Received 27 May 2024
Accepted 17 November 2024

Keywords:
“Vinegar syndrome”
Motion picture film degradation
De-acetylation
Cellulose acetate
Multi-analytical protocol
Preventive conservation

ABSTRACT

One of the most crucial subjects for cellulose acetate motion picture film conservation is associated with the so-called “vinegar syndrome”. This paper shows the set up of an innovative procedure for the artificial induction of this degradation process in both cellulose triacetate laboratory samples and real motion picture films. Moreover, a multi-analytical approach based on optical microscopy, gravimetry, solubility, free acidity measurements and tensile tests, combined with acetyl content calculation through Heterogeneous Saponification Method (HSM) and Fourier Transform InfraRed Attenuated Total Reflectance spectroscopy (FTIR-ATR) was also defined to obtain a complete picture of the evolution of the “vinegar syndrome”. The procedures presented in this paper are preliminary to the set up of new materials specifically tailored for the inhibition of the “vinegar syndrome”. The idea is to artificially induce the de-acetylation on cellulose acetate samples in a controlled, reproducible and non-aggressive way for the tested inhibitors, and monitor the evolution of the process through the abovementioned multi-analytical approach.

1. Introduction

The history of using cellulose acetate polymers as support for motion picture films is an interesting topic. Because of the instability and flammability of celluloid (i.e. cellulose nitrate), the film industry started to look for a safer alternative with similar physicochemical properties: during the first half of the XIX century, cellulose acetate (CA, cellulose diacetate, CDA, from the 1920s and cellulose triacetate, CTA, from the 1950s) was proposed as a good substitute [1–5]. Thanks to its lower flammability (flash point of 430 °C versus 4.4 °C of celluloid), motion picture films made of cellulose acetate are called *Safety Films*. Unfortunately, also CA showed significant instability and degradation issues and, during the 1960s and 1970s, more stable polyesters gradually replaced it.

Most chemical deterioration mechanisms affecting CA polymers can be ascribed to a phenomenon commonly known as “vinegar syndrome” [4]. The major chemical degradation reaction of CA concerns the cleavage of the ester bonds between the acetate group (CH_3COO) and the cellulose backbone through ester hydrolysis (de-acetylation), with the formation of hydroxyl groups and the release of acetic acid [3,4,6–11]. Indeed, the “vinegar syndrome” gets this name because of the characteristic smell emitted by degraded CA films. A model to describe the evolution of the “vinegar syndrome” in both naturally and artificially aged films [9,11–17] was proposed by the Image Permanence Institute [18] in the last decades of the XX century. It was found that de-acetylation is strictly influenced by temperature, relative humidity (RH) and pH (acid or alkaline). In particular, the formed acetic acid acts as a catalyst itself for the de-acetylation reaction and induces an autocatalytic process [18]. Past studies proposed a threshold value of the concentration of acetic acid for the onset of this process [9,18] but recent publications pointed out that it could be more correct to describe the de-acetylation process as an autocatalytic process occurring at all acid concentrations [19]. Indeed, the presence of acetic acid significantly decreases the activation energy of the first step of the reaction (about 20 kcal/mol). This reduction is the reason for the higher rate of the acid-catalyzed reaction path [20]. Many studies [21] also investigated a second hydrolysis process taking place during the degradation pathway and involving depolymerization due to cleavage of the glycosidic bonds of the CA backbone [4,22] with a consequent decrease in molecular weight. Moreover, to produce motion picture films, CA is typically modified with plasticizers that are commonly lost over time [23]. Then, the progressive depolymerization and loss of plasticizers lead to embrittlement and con-

* Corresponding author.
E-mail address: emiliano.carretti@unifi.it (E. Carretti).

https://doi.org/10.1016/j.culher.2024.11.013

sequent cracking of the material [22] compromising the usability of the motion picture film.

Based on this knowledge of the chemical mechanisms involved in the "vinegar syndrome", to prevent the trigger and promote the inhibition of this phenomenon, some possible methodologies have been studied [9,11–13,15–17,24]. Until today the most diffuse way is to act on parameters that determine its kinetics, i.e. humidity, temperature, and acidity [18,25–27]. The results of such investigations showed that the CA-based motion picture films should be stored at low temperatures and RH in a well-ventilated environment to promote the removal of the degradation by-products which can further catalyze the de-acetylation reaction of the backbone. Another promising approach concerns the subtraction of acetic acid from the environment to avoid the trigger of the autocatalytic process. For this purpose, two routes can be pursued: absorbing it or neutralizing it. Many solutions have already been studied, each with some positive and negative aspects [6,26–33]; the most promising systems seem to be the Metal-Organic Frameworks (MOFs) [34–36] but the main drawbacks are the high costs and the huge amount of time needed for their synthesis. On these bases, it would be interesting to pursue innovative routes, possibly exploiting new smart materials.

The analysis of current normative [37] showed that, before setting up new methodologies, it was important and urgent to define a proper protocol for the artificial induction of the "vinegar syndrome" to be used to test and evaluate the evolution of the syndrome with or without possible new inhibitors. Together with this new degradation procedure, it was mandatory to define also a multi-analytical protocol for monitoring both the induction of the "vinegar syndrome" and its subsequent evolution. From several studies conducted between the eighties and nineties [9,13,38,39], it was found that is possible to monitor the free acidity (i.e. the free acetic acid adsorbed inside the film) through an acid-base titration method [18,37,40,41] or through ion chromatography [22,23] and Solid Phase Micro Extraction – Gas Chromatography/ Mass Spectrometry (SPME-GC/MS) [42–44].

Another approach to defining the conservation status of CA media is based on the measurement of the substitution degree, which is the amount of the mass percentage of acetyl groups bound to the cellulose backbone. In the literature, some methodologies to quantify the acetyl content in motion picture films through different techniques (UV–vis spectrophotometry [10,45], Nuclear Magnetic Resonance NMR [21,46–48]) are reported. The weak point of these latest methods, which require the use of liquid analytes, is the dependence of the solubility of cellulose acetate on the degree of substitution. It is well known that cellulose acetates with a very low degree of substitution are very difficult to solubilize in most of the solvents commonly used for these analyses [49]. In addition, all the abovementioned methods are invasive and/or destructive. Recently, Infrared Spectroscopy, in particular ATR or μ-FTIR, has been used to define the degree of substitution of cellulose acetate by means of a non-invasive or micro-destructive protocol [46,49]. On the other hand, FTIR methods for analyzing the degree of substitution can run into problems as spectral resolution diminishes as the CA degrades, making quantitative analysis less accurate [47].

In this work, in addition to a degradation method to trigger the "vinegar syndrome" in motion picture films, a multi-analytical protocol has been proposed to collect analytical data to define, by means of several different measured properties, the real extent of the degradation processes in the various steps of the induction and evolution of the syndrome.

2. Research aims

According to the state of the art concerning the "vinegar syndrome" in motion picture films made of CA reported in the **Introduction** section, two main research aims were individuated for the present study. Bearing in mind that one of the main goals of the actual research in this field is to develop innovative methodologies for inhibiting and preventing the "vinegar syndrome" through the proposal of innovative smart materials, the first aim was to set up a new way to artificially induce this phenomenon, for evaluating the performance of these new systems. With a view to testing smart materials – our team is working on polymeric systems made of polyamines that could be potentially useful to stop the de-acetylation process and prevent further deterioration of cellulose acetate films –, it is fundamental to set up an innovative method to artificially induce the "vinegar syndrome", that can be used in the presence of such inhibitors without damaging them and especially without adopting high temperature (i.e. we need to work at room temperature or, in any case, below 30 °C). This goal was particularly complex since the methods commonly used to induce the "vinegar syndrome" are based on the conditioning of the samples at high temperatures for some days [9,17,20,37]. As indicated in the literature, one of the methods commonly used to artificially induce the "vinegar syndrome" in real motion picture films made by CA (RMPF), has been proposed by the *Image Permanence Institute* [9,17] and subsequently reported in the ISO 18901:2010 [37]. This method involves heating up for 72 h at 100 ± 2 °C a certain amount of RMPF in a sealed metal-foil bag. Processing the films in this way shows an increase in free acidity and a loss in tensile properties and emulsion [41]. It is evident that these methods which are based on conditioning the samples at high temperatures for many hours can strongly compromise the chemical stability and the performance of polymeric inhibitors like those above mentioned. Therefore, the possibility to induce the de-acetylation process through a procedure that is realized at room temperature and is able to successfully test the performance of polymeric inhibitors by safeguarding their stability, at today is still not considered. Then, the first aim of this work is the set up of a room temperature procedure to artificially induce the "vinegar syndrome" on lab CTA-based film (LCBF) and then on RMPF. The artificial induction of the de-acetylation process was set up by a method able to achieve controllable and reproducible results. It is important to mention that a protocol to test possible inhibitors and preventing agents for the "vinegar syndrome" should consist of two steps: the first step, which can adopt also strong conditions, is the one to induce the de-acetylation; the second step is used to restart the de-acetylation reaction after applying the inhibitor and needs to be conducted at room temperature to avoid the chemical degradation of the polymeric system. We worked both on pure LCBF and RMPF because examining pure LCBF allowed to analyse the effects of the artificial induction of the de-acetylation process of pure CA, without considering the effects of plasticizers and emulsion layer. Moreover, the protocol had to induce the de-acetylation process on samples with reasonable kinetics compatible with lab timelines to appreciate and study its evolution and to be compatible with possible innovative thermosensitive inhibitors [4,18].

The second aim of this work was the setting up of a multi-analytical protocol that allows following the evolution of the artificially induced de-acetylation of the films by focusing the attention on both their chemical (substitution degree of the polymers and free acidity) and the mechanical properties (tensile stress resistance). By comparing normalized results referred to the same phenomenon (i.e. the de-acetylation process) but obtained by different methodologies and by proving their coherency, was possible to demonstrate the occurrence of the de-acetylation reaction but also to validate our multi-analytical method. In addition, a wide overview in terms of properties variation (both chemical and mechanical) induced by the degradation protocol was collected.

3. Experimental section

Chemicals and materials are reported in Paragraph 1.1 of the SI (Fig. SI1 and SI2).

3.1. The artificial induction of the de-acetylation process

An innovative method for the artificial induction of the "vinegar syndrome" based on the exposure of LCBF and RMPF to a high-acidity atmosphere was proposed in this work and called the "high acidity induction method". It is well known that the deterioration of CTA films by de-acetylation can be induced by acid or basic substances [50,51]. Therefore, the effects of the exposure to HCl-saturated atmospheres on both LCBF and RMPF were evaluated (degradation protocol "HCl5"). The samples were exposed to a saturated atmosphere of HCl 5 M in airtight chambers (volume ca. 130 mL) at different times at 25 ± 3 °C. The RMPF and LCBF were cut into fragments of 50 × 16 mm (total amount for each chamber ca. 1 g and hung at the top of the chamber with a Teflon wire, spaced out with glass marbles with a diameter of about 2 mm to avoid their mutual contact during the storage. A vial with 8 mL of HCl 5 M was placed at the bottom of the chamber (see Fig. SI3, Paragraph 1.2 of SI). LCBF were exposed to this HCl atmosphere for up to 16 days (with a sampling every two days), while for RMPF the degradation period lasted up to 30 days (with a sampling every 3, 6, 9, 12, 15, 20, 25, 30 days). In both cases, each sampling corresponded to a different airtight chamber to avoid interruption of thermo-hygrometric conditions; this meant that for these experiments the number of chambers corresponded to the number of samplings. The environmental conditions (temperature and relative humidity) were monitored hourly with a data logger.

A second degradation protocol to artificially induce the "vinegar syndrome" (degradation protocol "ATM2.X") was set up by adding two further steps after the HCl treatment: after the first step (exposure to a saturated atmosphere of HCl 5 M in 130 mL airtight chambers at 25 ± 3 °C for 3 days, LCBF and 9 days for RMPF), the samples were kept out of the chamber and left for 24 h under hood at 50 RH% at room temperature (25 ± 3 °C) to eliminate the excess of adsorbed HCl; then the samples were stored again in the same airtight chambers at 100 RH% and 25 ± 3 °C for 12, 24, 36, 48 days to monitor the further evolution of the de-acetylation reaction. This protocol is labeled ATM2.X where X indicates the duration, in days, of the exposure to a saturated atmosphere of HCl 5 M (then we have ATM2.3 protocol for LCBF and ATM2.9 protocol for RMPF).

The use of HCl in the first step of the artificial degradation protocol proposed in this study with respect to the traditional ones (consisting of keeping the samples at high temperature for many hours) introduces a strong chemical agent that for the purpose of this paper (see Research Aims section) does not create any problems. It is obvious that the approach proposed in this study is not aimed to substitute the traditional methods, but has the great advantage, as we will show, of being considered an optimum method to test possible inhibitors for the "vinegar syndrome".

3.2. Analytical techniques

3.2.1. Optical microscopy

Optical microscopy analyses were performed in transmission mode with a Reichert optical microscope (Austria) coupled with a Nikon Digital-Sight DS-U3 camera; images were acquired at two different magnifications with the *epi* 5.5 (20x) and *epi* 11 (40x) lenses and were digitized with the NIS-Elements software.

3.2.2. Solubility tests

A first, rough evaluation of the variation in the acetyl content during the artificial induction of the de-acetylation was carried out through solubility tests. Table SI1 (Paragraph 1.2 of SI) shows the solubility of cellulose acetate in different solvents by varying its acetyl content [4,52,53]. 60 mg of sample was cut into little fragments in the order of a few mm^2 and dispersed in 3 mL of the chosen solvent. The extent of solubilization was assessed qualitatively after 48 h.

3.2.3. Ion chromatography (IC)

Samples of LCBF and RMPF were cut into little fragments and maintained in water under stirring for 24 h at 38 °C. The extracts were analyzed with an ICS-90 Ion Chromatography Sistem (Dionex), using Na_2CO_3 and $NaHCO_3$ 1.8 mM solution as buffer and H_2SO_4 10 mM as suppressor and working at 8 bar pressure.

3.2.4. Gravimetry tests

We investigated if the variation in weight during the artificially induced "vinegar syndrome" could be associated with the de-acetylation process. Weight loss in percent (WL%) was calculated as follows:

$$WL(\%) = [(W_t - W_o)/W_o] \times 100 \quad (1)$$

where W_o is the initial weight of the sample (g) and W_t is the weight of the sample at time t of the artificial aging. Since the samples adsorbed water during the storage in the chambers, the W_t-values reported in the graphs as a function of aging time were taken 24 h after their removal from the chambers keeping them under the hood at 25 ± 3 °C and 50 ± 5 RH% to reach equilibrium. The reported results were the average values calculated between three samples with the corresponding standard deviations.

3.2.5. Free acidity measurements

To estimate the free acidity (which corresponds to the free acetic acid that was adsorbed onto the support, i.e. the unesterified organic acid in the ester) a method reported on the ASTM D 871-96 normative [40] was used with some modifications. More details are reported in Paragraph 1.3 of SI. The percentage of acidity as free acetic acid has been calculated as follows:

$$\text{Free acidity}(\%) = [(A - B) \times N \times 0.06 \times 100]/W \quad (2)$$

where: A = volume of NaOH solution used to titrate the sample (mL), B = volume of NaOH solution used to titrate the blank (mL), N = normality of the NaOH solution, and W = weight of sample (g). The reported results were the average values calculated between three samples with the corresponding standard deviations.

3.2.6. Combined acetyl or acetic acid content calculation through the heterogeneous saponification method (HSM)

A method based on Heterogeneous Saponification and reported on the ASTM D 871-96 normative [40] was used with some modifications (more details are reported in Paragraph 1.4 of SI). This procedure allowed to measure the total amount of acetyls bound to the cellulose backbone and the free acidity adsorbed by the polymeric network. The percentage of combined acetyl or acetic acid content was calculated as follows:

$$\text{Acetyl or acetic acid}(\%) = [(D - C) \times N_a + (A - B) \times N_b + P] \times (F/W) \quad (3)$$

where: A = volume of NaOH solution required for titration of the sample (mL), B = volume of NaOH solution required for titration of the blank (mL), N_b = normality of the NaOH solution, C = volume of HCl required for titration of the sample (mL), D = volume of HCl required for titration of the blank (mL), N_a = normality of the HCl solution, F = constant 4.305 for acetyl, W = weight of sample (g). The reported results are the average values calculated between three samples with the corresponding standard deviations.

3.2.7. Acetyl content with FTIR-ATR spectroscopy

To evaluate the decrease in the acetyl content on RMPF in a non-invasive and non-destructive way, we performed FTIR-ATR spectroscopy before and after the de-acetylation induction. The FTIR spectra were collected with an IRAffinity-1S Fourier Transform Infrared Spectrometer (Shimadzu) by using the MIRacle Single Reflection Horizontal ATR Accessory equipped with a Diamond/ZnSe Performance flat tip Crystal Plate. The resolution was 2 cm^{-1}, the number of scans was 64 and the range 4000–600 cm^{-1}. For comparison, the spectra were adjusted to the same baseline and normalized on the peak at 1030 cm^{-1} [46,49].

The following ratio was calculated:

$$\left[\text{Intensity of a diagnostic peak}\left(\text{arbitrary units}\right)\right] / \left[\text{Intensity of the 1030 cm}^{-1}\text{ peak}\left(\text{arbitrary units}\right)\right] \quad (4)$$

The peak at 1030 cm^{-1} was chosen as the reference peak (i.e. internal standard): it is assigned to the C–O–C stretching vibration of the anhydro-glucose ring and it was assumed not to vary during the degradation protocol [46,49]. As probe peaks, able to monitor the evolution of the de-acetylation, the following peaks, whose intensity is assumed to change during the de-acetylation process (see Fig.SI4, Paragraph 1.5 of SI), were selected: (i) the peak at 1220 cm^{-1} assigned to the C–O stretching of the acetyl group; (ii) the peak at 1730 cm^{-1} assigned to the C=O stretching of the acetyl group; (iii) the peak at 3330 cm^{-1} assigned to the O–H stretching. For each sample of LCBF film and RMPF, five spectra were collected in different areas; the average values and the standard deviations were reported.

3.2.8. Tensile tests

Tensile tests were performed on RMPF (5 × 1 cm) before and after the induced degradation process to evaluate how mechanical properties varied during this test. Measurements were carried out using a Discovery HR-3 rheometer (TA Instruments) in a tension fixture mode, setting a loading gap of 2 cm and applying an axial force up to 40 N with a rate of 94 µm/s. The maximum axial force applied to the films was 40 N because this value corresponded to the upper limit of the tensile stress of the instrument. For each sample, the measurements were performed in four replicas and the calculated media and standard deviation were reported. More details about the asset of the measurement and the calculation of Young's Modulus are reported in Paragraph 1.6 of SI. Tensile tests were carried out only on real motion picture films because they had uniform shape and thickness (125 ± 3 µm), while standard cellulose acetate laboratory films showed a strong variability in both the shape and the thickness (130 ± 20 µm), which strongly affected the significance of the results associated with this test.

3.2.9. Thermogravimetric analysis (TGA)

Tests were performed on RMPF in a nitrogen atmosphere at a heating rate of 10 °C/min over a temperature range of 25–500 °C, with an initial sample weight of approximately 5 mg using an SDT 650 thermal analyzer (TA).

4. Results and discussion

4.1. The induction of the "vinegar syndrome" by the high acidic induction method (HCl5M) on lab CTA-based films

The samples subjected to this degradation protocol were first exposed to a saturated atmosphere of HCl 5 M for 2, 4, 8, 10, 12, 14, 16 days for the LCBF and for 3, 6, 9, 12, 15, 2, 25, 30 days for the RMPF. The longer times adopted for RMPF were selected to have comparable effects with LCBF (vide infra). The results obtained for the LCBF and RMPF will be discussed separately.

4.1.1. Gravimetry tests and free acidity measurements

Gravimetry data are reported in Fig. 1A and indicate a progressive weight loss of the samples during the test. For the first six days of exposure to HCl 5 M atmosphere, the decrease in weight is low (2.97 ± 0.01 wt%) and started to increase more rapidly after the sixth day (9.1 ± 0.4 wt%) up to a loss of 32 ± 2 wt% after sixteen days. Concerning the free acidity, it was possible to appreciate an increase of the free acidity (Fig. 1B) from 0.06 ± 0.01 % (not degraded) up to 3.2 ± 0.2 % (16 days). Obviously, it was an opposite trend compared to both the weight loss (Fig. 1A) and the acetyl content (Fig. 1C).

4.1.2. Acetyl content via HSM

As discussed in the Experimental section, a protocol based on ASTM D 871–96 was used to measure the acetyl content for each sample [40]. This procedure cannot discriminate between the acetyl content (the acetic acid esterified onto the cellulose backbone of the polymer) and the free acidity (given by the unesterified acetic acid physisorbed by the film). Therefore, to better evaluate the actual acetyl content, the free acidity values reported in Fig. 1B were subtracted from the acetyl content values obtained via HSM. In Fig. 1C, acetyl content with (red line) and without (black line) the subtraction of the free acidity is reported: it was evident that the correction is more important for samples exposed to the HCl atmosphere for longer periods. It was interesting to notice that the acetyl content change had the same trend of the weight loss: the acetyl content decreased very slowly from 45 ± 1 % (not degraded) to 37.5 ± 0.3% in the first six days and more rapidly afterward up to 4.9 ± 0.5% after 16 days of contact with the HCl atmosphere. Comparing the correct acetyl content obtained with the HSM with the values reported in Table SI1 (Paragraph 1.2 of SI), it was possible to make the following considerations:

- Before the degradation protocol the value of the acetyl content is 45 ± 1 %, which is typical of CTA (range of acetyl content 44.8–43.0 %);
- the samples at 2 (41.4 ± 0.2 %), 4 (37.84 ± 0.03 %), and 6 days (37.5 ± 0.3 %) were classifiable as CDA (range of acetyl content 42.9–34.9 %);
- the samples at 8 (29.8 ± 0.7 %) and 10 days (23 ± 2 %) were ascribable to CMA (range of acetyl content 34.9–21.1 %);
- the samples at 12 (13.1 ± 0.2 %), 14 (11.2 ± 0.4 %), and 16 days (4.9 ± 0.5 %) were classifiable as "0″-CA (acetyl content ≤ 21.1 %) [52].

Moreover, the solubility trend of the samples (Table SI1 in Paragraph 2.1 of SI) was coherent with the correct acetyl content calculated via HSM.

4.1.3. Acetyl content with FTIR-ATR spectroscopy

Even if the HSM method was able to provide useful information about the decrease in the acetyl content induced by the degradation protocol, the sampling of the film was mandatory. For this reason, we proposed also a non-destructive and non-invasive method to monitor the de-acetylation process based on the use of FTIR-ATR Spectroscopy. In Fig. SI5 (Paragraph 2.2 in SI) the spectra of all the LCBF subjected to the HCl5M degradation protocol are reported. Coherently with the data obtained from the previous analyses (Fig. 1), the intensity of all the peaks associated with the acetyl group bound to the cellulose backbone of the CA (at 1220, 1340 and 1750 cm^{-1} attributed to the C–O stretching, the C–H bending of the CH_3 and the C=O stretching, respectively [49,54]) tended to decrease by increasing the duration of the exposure to the HCl atmosphere (Fig. SI5B of Paragraph 2.2 in SI). Moreover, a light shift of the peak at 1030 cm^{-1}, associated with C–O–C stretching of the glycosidic ring [49,54] to lower wavenumbers (1018 cm^{-1}), was observed after 16 days together with the formation of two shoul-

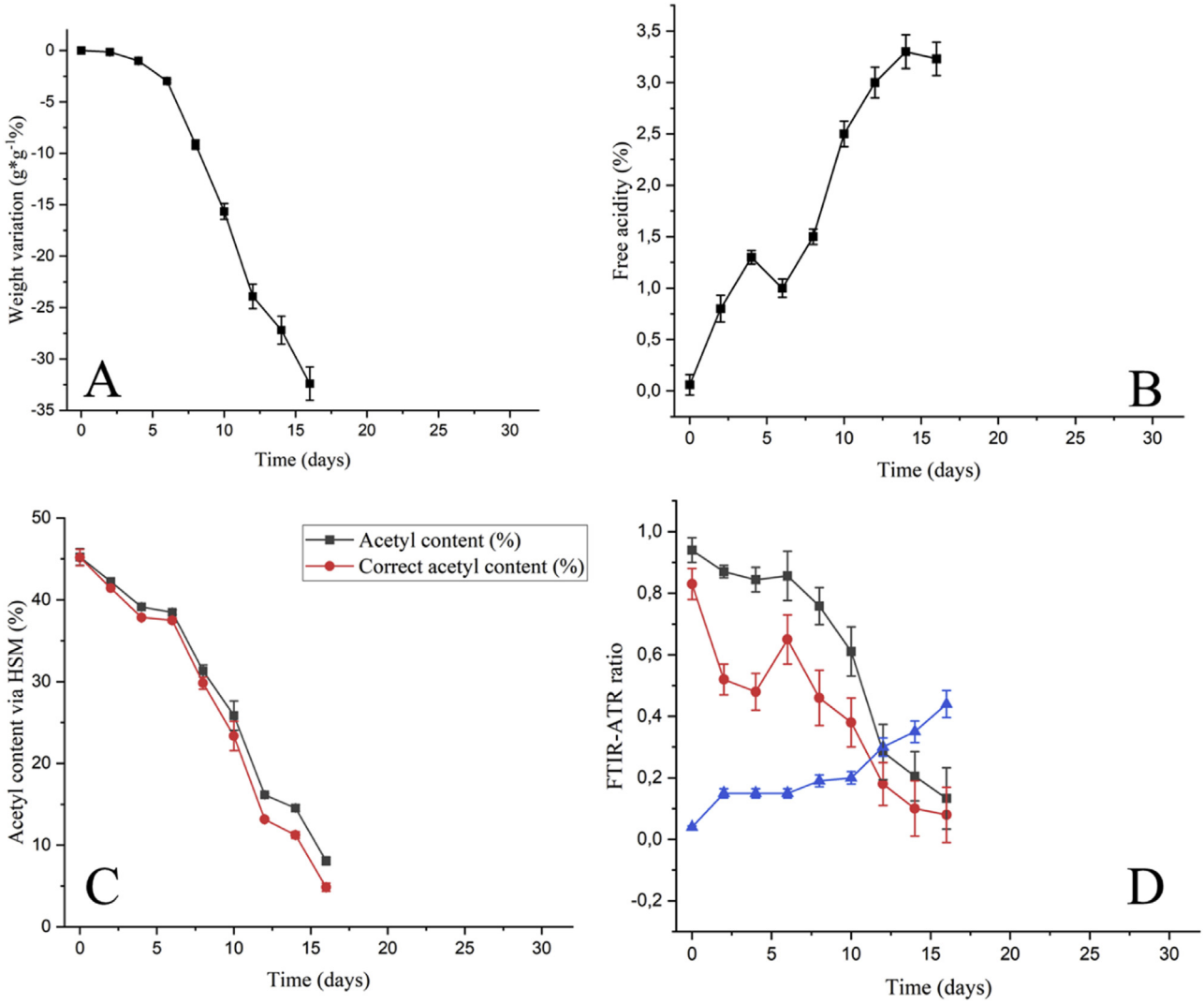

Fig. 1. (A) Weight loss (%), (B) free acidity (%), and (C) acetyl content measured via HSM (%) with (red) and without (black) the correction through free acidity data, for LCBF film as a function of the time of exposure to HCl 5 M saturated atmosphere. The results of each measurement are expressed as the average value and the corresponding standard deviation calculated for three fragments of the same film subjected to the same degradation protocol. (D) FTIR-ATR ratios I_{1220}/I_{1030} (black), I_{1750}/I_{1030} (red) and I_{3330}/I_{1030} (blue) as a function of degradation time; the results of each measurement are expressed as the average value and the corresponding standard deviation calculated from five spectra acquired in different areas of the film subjected to the same degradation protocol.

ders at 1064 and 1108 cm^{-1} [55], indicating an alteration also of the cellulose backbone. At the same time, the broad peak associated with the OH stretching at 3330 cm^{-1} tended to increase with the duration of the test (Fig. SI5C of Paragraph 2.2 in SI). On these bases, the evolution of the de-acetylation process induced by high acidic exposure was followed by studying the trend of the ratios I_{1220}/I_{1030}, I_{1750}/I_{1030} and I_{3330}/I_{1030} as a function of time (1220, 1030, 1750, and 3330 indicate the position of the diagnostic peaks in cm^{-1}, Fig. 1D). The progressive decrease of the intensity of the peaks at 1220 and 1750 cm^{-1} is evidence of the de-acetylation process induced by the HCl atmosphere. Whereas for the trend of the intensity of the 3330 cm^{-1} peak (whose increase is coherent with the occurrence of the de-acetylation reaction) is not possible to exclude a contribution of the moisture adsorbed by the film due to the high RH of the environment (i.e. the airtight chambers where the degradation test was carried out). Indeed, the water absorption could affect the intensity of the peak at 3330 cm^{-1}, which is associated with the stretching of the O–H group. In addition, the increase in the polarity of the system with the progress of de-acetylation increase also the capacity to absorb water, which is very high for pure cellulose.

4.2. The induction of the "vinegar syndrome" by the high acidic induction method (HCl5M) on real motion picture films

The most important differences in the effects of the HCl5 degradation protocol on the RMPF, in comparison with the LCBF are evident in the images reported in Figs. SI6 and SI7 (Paragraph 2.3 of SI).

In detail, Fig. SI6 shows macroscopic signs of degradation: the film started to deform and curl because of the reduction in the size of the cellulose acetate support (the so-called "channeling" phenomenon) [1,2]. At the same time, the emulsion started to be very sticky and detached easily from the support [56], as it was possible to appreciate from the optical microscopy micrographs reported in Fig. SI7B. Micrographs reported in Figures SI7C, SI7D, and SI7E collected from the surfaces of the samples treated 15, 20, and 30 days showed the presence of needle-shaped crystals and microbubbles, probably due to the exudation of plasticizers [57] and/or low molecular weight fragments or other film components aggregating/crystallizing. In particular, the needle-shaped crystals could be associated with triphenyl phosphate, while the microbubbles with phthalates [57,58]. The presence of plasticizers

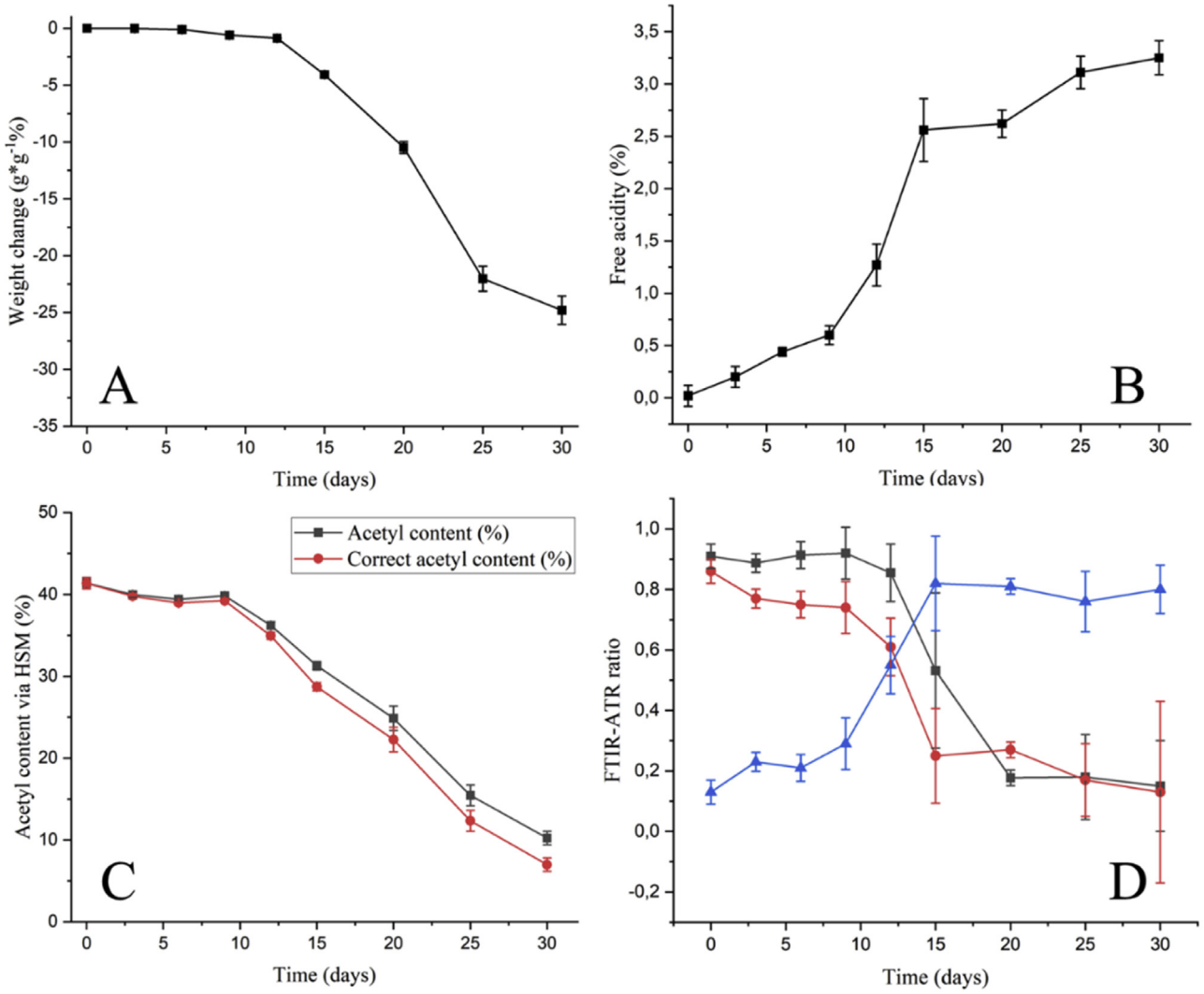

Fig. 2. (A) Weight loss, (B) free acidity and (C) acetyl content with (red) and without (black) the correction with the free acidity calculated via HSM for the HCl5M RMPF as a function of time exposure. The results of each measurement are expressed as the average value and the corresponding standard deviation calculated for three fragments of the same film subjected to the same degradation protocol; (D) FTIR-ATR ratios I_{1220}/I_{1030} (black), I_{1750}/I_{1030} (red) and I_{3330}/I_{1030} (blue) as a function of degradation time; the results of each measurement are expressed as the average value and the corresponding standard deviation calculated from five spectra acquired in different areas of the film subjected to the same degradation protocol.

(both triphenyl phosphate and phthalates) was confirmed in the FTIR spectrum reported in Fig. SI9 (A) and commented in the Supporting Information (Paragraph 2.4).

4.2.1. Gravimetry tests and free acidity measurements

The weight loss during the degradation process was monitored and the results are shown in Fig. 2A. The decrease in weight was not visible for the first 12 days of exposure to the HCl atmosphere, while in the following 18 days, the weight decreased up to 25 ± 1 %. So, comparing the results of the gravimetry tests of LCBF and RMPF, it was evident that the weight loss was both lower and slower for the latest ones. The explanation of this phenomenon could be traced back to what has been reported in previous studies on the properties of the emulsion in real motion picture films [50,51]. It has been highlighted that the emulsion acts as a protective barrier being able to partially neutralize the acetic acid [50] and therefore slow down the de-acetylation kinetics in the cellulose triacetate-based support. Moreover, it has been shown [51] that the gelatin emulsion layer imparts some degree of stability to CA film base due to its ability to scavenge and neutralize the acetic acid and partially prevent the diffusion of oxygen into the film. Finally, it is well known [2,32] that the gelatine-based emulsion is strongly hygroscopic and is able to absorb moisture; then, it is reasonable to assume that a part of the weight recorded post-exposure, especially for the more degraded samples, was attributable to the presence of retained water in the residues of the emulsion layer. Concerning the free acidity (see Fig. 2B), it increased during the degradation protocol, starting from a value of 0.02 ± 0.01 at time 0 days up to a value of 3.25 ± 0.2 after 30 days of storing in the HCl 5 M atmosphere. This value was equal to the one reported for LCBF after 16 days (3.23 ± 0.2 %, see Fig. 1B), showing that the amount of free acidity emitted by LCBF was identical to the one emitted by RMPF after being exposed to the same conditions twice as long. This was probably due to the stabilization effect of the emulsion layer. In the case of free acidity too, a variation in the emission rate of acetic acid is detected on the 9th day of the experiment.

4.2.2. Acetyl content via HSM

The acetyl content calculated through the HSM and corrected by the free acidity is reported in Fig. 2C. If we compare this graph with that shown in Fig. 1C for LCBF, the trend of the slope of the

curve indicates that the de-acetylation process starts after 9 days (vs 6 days of the LCBF). Moreover, afterward, the degradation process is slower as indicated by the slope of the curve of RMPF which is much lower than the one of LCBF. In detail, it was possible to appreciate that the time needed to reach the same degree of acetyl content was almost double (30 days versus 16, Figs. 1C and 2C). A similar trend was observed also for weight loss (see Figs. 1A and 2A).

4.2.3. FTIR-ATR spectroscopy

The FTIR-ATR spectrum of RMPF before the HCl5 treatment (see Fig. 8SI and 9SI in Paragraph 2.4 of SI) provided information about the chemical nature of both the support (made of CA) and of the emulsion layer that is composed of a protein, probably collagen. A more detailed comment in this sense is reported in Paragraph 2.4 of SI. To follow the degradation treatment by HCl5, the FTIR-ATR analysis was carried out only on the back side of the RMPF (i. e. the support side) in order to avoid interferences given by the signals of the emulsion layer. Using the same approach as reported for LCBF in Fig. 1D, the results obtained for RPMF were collected in Fig. SI10 (Paragraph 2.5 of SI) and 2D. Also in this case, the results matched those obtained with other analytical techniques reported in Fig. 2A, B and C, confirming that the treatment HCl5 was a good way to artificially induce the "vinegar syndrome" also in RMPF, even if with different kinetics and a longer induction period in comparison with LCBF.

4.2.4. Tensile tests

In RMPF we also evaluated the progressive alteration of the mechanical properties of the film induced by the degradation protocol. This is a key point, being the usability of the film strictly related to its mechanical resistance and elasticity. In Fig. SI11A and B (Paragraph 2.6 in SI), the trend of the Axial Force versus Strain and the Young's Modulus (E, eq. SI1, Paragraph 1.6 in SI) versus time (in days) of exposure to HCl were plotted. A well-defined trend was evident: as the exposure time increased, the slope of the curve Axial force versus Strain decreased and, consequently, also the value of E (from 15 ± 1.5 MPa at time = 0 up to 9.8 ±.8 MPa at time = 25 days); this meant that samples subjected to the same stress underwent greater deformation as the degradation process went ahead. Further confirmation of the loss in tensile strength was the fact that the sample after 15 days underwent permanent plastic deformation at 39.5 ± 3 N, while specimens after 20 and 25 days broke at about 35±3 N and 32±4 N, respectively. This point confirmed that, after 20 days of exposure to the HCl atmosphere, the films reached an advanced state of degradation, with a consequent strong reduction of the tensile strength. The decrease in mechanical resistance could be due to the depolymerization of the support. In fact, the formed acetic acid and the adsorbed HCl probably induced the hydrolysis of the glycosidic bonds between the monomeric units of the polymeric backbone with a consequent lowering in the average molecular weight. This effect is clearly indicated by the profile of the differential thermogravimetric analysis (DTG) curves of the RMPF shown in Figure SI12 (Paragraph 2.6 in SI) where a shift of the pyrolysis from ca. 400 °C (sample P0) to lower values is observed (P20 and P25) [59].

Moreover, recently [20] it was found that CA films that include plasticizers, triphenyl phosphate or diethyl phthalate, degrade 2.5x and 3x times faster than the pure polymer, respectively. In our study, an opposite trend is observed by comparing LBCF and RMPF but it is important to point out that the degradation protocol adopted by Mohtar et al. (2021) is different and includes exposure of the films to high temperature (70 °C) for several weeks. In addition, they conducted artificial aging tests on laboratory samples without an emulsion layer, which has a stabilization effect [50,51] and plays an important role in the degradation process due to its capacity to retain both acid and moisture. Anyway, more detailed and in-depth studies will be needed to better evaluate the effect of plasticizers on the kinetics of the degradation protocol proposed in this work.

4.3. The evolution of the "vinegar syndrome" induced by HCl 5 M by storing at room temperature and high RH for both LCBF and RMPF (ATM2.X degradation protocol)

As reported in the Research aims section, once ascertained that the HCl 5 M atmosphere succeeded in inducing the de-acetylation process, it was fundamental to set up an innovative procedure to stop and re-start the "vinegar syndrome" in order to follow its evolution after the addition of an inhibitor. In order to safeguard the chemical-physical stability of a polymeric inhibitor, it is fundamental to split the degradation protocol into two steps: the first one, more "aggressive", to induce the de-acetylation of the support through the exposition of the films to HCl vapors, and the second one, more "soft", to promote the evolution of the de-acetylation process with and without the inhibitor in order to test its efficacy. First of all, two main problems had to be solved: (i) deciding when stopping, in terms of days of exposure, the HCl5 treatment to have only the induction of the "vinegar syndrome", without a too-boosted de-acetylation, and (ii) avoiding possible excess of adsorbed HCl onto the LCBF and RMPF. The criterion for solving the first problem was to stop the HCl5 after 3 days for LCBF (see Fig. 1) and 9 days for RMPF (see Fig. 2). The duration of HCl5 exposure for RMPF was calculated considering the change in the slope of the curve in Fig. 2B and C; for LCBF we chose 3 days as duration of HCl5 exposure in order to have a CA film with a starting acetyl content similar to the one calculated for the initial RMPF. This difference was adopted due to the already observed slower kinetics for RMPF compared to LCBF, considering also the higher rate of free acidity emission of LCBF than RMPF.

4.3.1. Ion chromatography

The amount of CH_3COOH and HCl adsorbed onto both LCBF and RMPF samples was determined by IC, measuring the concentration of chloride and acetate ions before and after the exposure to HCl atmosphere (lasted 3 days for LCBF and 9 days for RMPF): the results are reported in Table 1. The presence of these species in both the LCBF and RMPF also before the degradation protocol is probably due to residues of the casting solvent (chlorides) and to an incipient de-acetylation process (acetates). An increase in both acetate and chloride ions is detected after the exposure, demonstrating the presence of free HCl and CH_3COOH into the RMPF. To eliminate these volatile compounds, both LBCF and RMPF were stored 24 h under hood at room temperature (RT) and RH ca. 50 %. The data reported in Table 1 indicate that the concentration of chlorides and acetates strongly decreased. The greater desorption of HCl compared to CH_3COOH during equilibration at room temperature and RH ca. 50 % for 24 h was due to the higher vapor pressure of the HCl that is >2700 times the one of the acetic acid (i.e. 4200 kPa versus 1.54 kPa at 21 °C).

By comparing the IC data obtained for the RMPF and the LCBF it was possible to observe that the concentration of chlorides and acetates was higher for RMPF, probably because of the presence of the emulsion layer that acts as an adsorber for both HCl and CH_3COOH. The above-described equilibration procedure was considered sufficient to eliminate the most of HCl. The fact that both a consistent amount of acetic acid and a much lower quantity of HCl (see last two columns of Table 1) remained in the samples could be considered a positive aspect, in the view that it could be a triggering factor for the subsequent re-starting and evolution of the "vinegar syndrome".

Table 1
Concentration of chloride and acetate anions in LCBF RMPF as a function of HCl exposure and subsequent equilibration for 24 h at room temperature and RH ca. 50%.

	[Cl⁻] and [CH3COO⁻] (mg/L)				
Samples	No exposure HCl	3 (CTA) or 9 (RMF) days of exposure to HCl	After 24 h RT and RH ca. 50 %	$[Cl^-]_{tc^{**}}/[Cl^-]_{fc^*}$	$[CH_3COO^-]_{tc^{**}}/[CH_3COO^-]_{fc^*}$
LCBF	$[Cl^-]$= 2.53 $[CH_3COO^-]$ = 0.98	$[Cl^-]$= 24.79 $[CH_3COO^-]$ = 291.78	$[Cl^-]$= 11.32 $[CH_3COO^-]$ = 220.10	4.5	224.6
RMPF	$[Cl^-]$ =9.32 $[CH_3COO^-]$ = 12.88	$[Cl^-]$ = 71.49 $[CH_3COO^-]$ = 306.57	$[Cl^-]$ = 25.78 $[CH_3COO^-]$ = 252.88	2.8	19.6

*fc: first column **tc: third column.

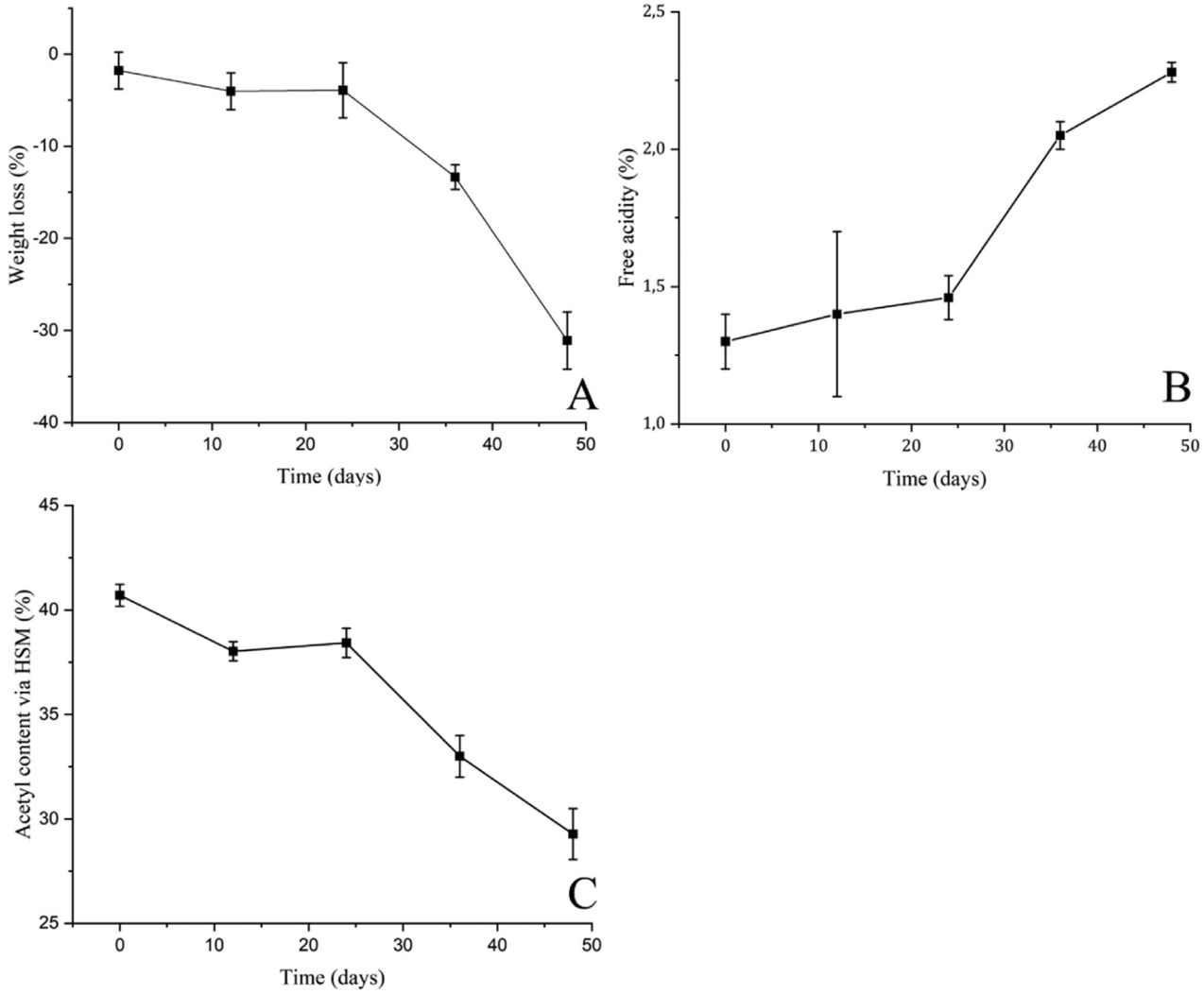

Fig. 3. (A) Weight loss, (B) free acidity and (C) correct acetyl content calculated via HSM reported for LCBF subjected to the degradation protocol ATM2.3 (i.e. first treated by HCl 5 M for 3 days, then equilibrated for 24 h at room temperature and RH ca. 50 %, and finally exposed to room temperature and RH = 100 %). On the x-axis the time of exposure to RH = 100% and room temperature during the third step of the treatment. The results of each measurement are expressed as the average value and the corresponding standard deviation calculated for three fragments of the same film subjected to the same degradation protocol.

Remembering to adopt soft conditions to follow the evolution of the syndrome and to safeguard possible tested inhibitors, the third step of the protocol developed in the present study was adjusted in the following way: samples were put in airtight chambers at room temperature with a 100 % RH for different periods (12, 24, 36, 48 days) to further carry on the de-acetylation thanks to the acetic acid formed during the first step (and the residual HCl), which acted as a catalyst for the reaction. The times were longer than for the first step of HCl exposure due to the weaker environmental conditions.

In all the kinetic curves reported in Figs. 3-6 the time 0 corresponds to LCBF and RMPF subjected for 3 and 9 days to the degradation protocol HCl5 and 24 hrs at RT and RH ca. 50 %, respectively.

4.3.2. Gravimetry tests, free acidity measurements and acetyl content via HSM

The results of the monitoring of weight loss (%), the free acidity (%), and the acetyl content measured via HSM (%) during the evolution of the degradation process induced by HCl 5 M and

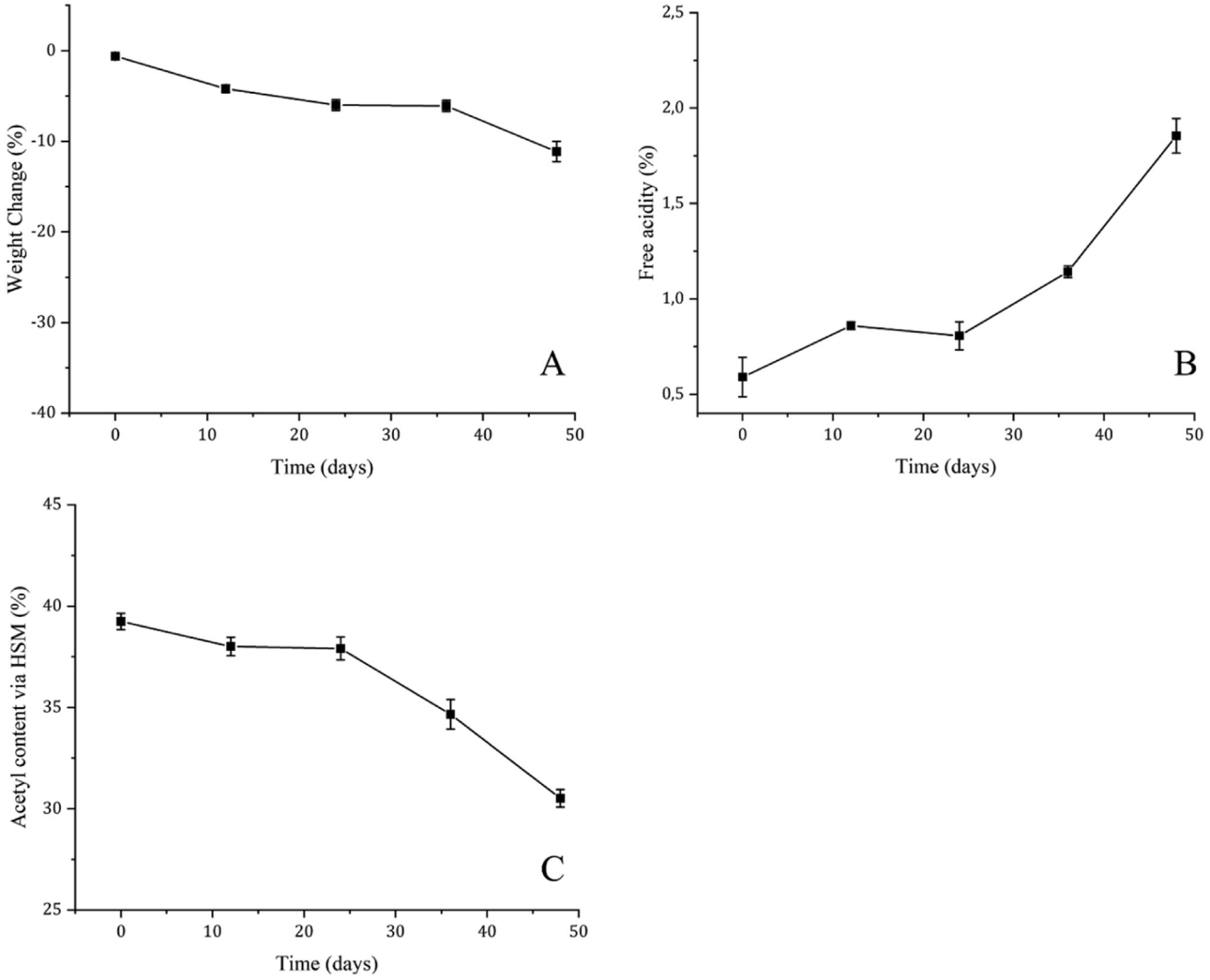

Fig. 4. (A) Weight loss, (B) free acidity and (C) correct acetyl content calculated via HSM reported for RMPF subjected to the ATM2.X (exposure to a saturated atmosphere of HCl 5 M for 9 days, then equilibrated for 24hours at room temperature and RH ca. 50 %, and finally exposed to room temperature and RH = 100 %). The x-axis indicates the time of exposure to RH = 100% and room temperature after the previous two steps of the treatment. The results of each measurement are expressed as the average value and the corresponding standard deviation calculated for three fragments of the same film subjected to the same degradation protocol.

by storing at room temperature and high RH (ATM2.X degradation protocol, where X indicates the duration, in days, of the HCl5 treatment) are reported in Figs. 3 and 4 for LCBF and RMPF, respectively.

It was evident that, after an induction period of about 24 days, the de-acetylation process starts again although at a much slower speed than the one induced by the HCl5 treatment (Fig. 1). This is confirmed by both the slower increase of free acidity (from 1.46 ± 0.08 % for F24_ATM2.3 to 2.28±0.04 % for F48_ATM2.3) and by the slower decrease of the total acetyl content (from 38.0 ± 0.5 % for F24_ATM2.3 to 29±1 % for F48_ATM2.3). This result indicates that we succeeded in inducing the "vinegar syndrome" in a controllable and soft way. This is a very important result in the view of the application of this degradation protocol to degraded RMPF in the presence of potential inhibitors, whose stability can be affected by the high acidity of the atmosphere typical of the HCl5 treatment. Similar results were obtained also with RMPF (Fig. 4, increase in the free acidity from 0.81±0.07 % for P24_ATM2.9 to 1.85±0.09 for P48_ATM2.9 and a decrease in the acetyl content from 37.9 ± 0.6 % for P24_ATM2.9 to 30.5 ± 0.4 % for P48_ATM2.9).

4.3.3. FTIR-ATR spectroscopy

Similar results were also obtained by the analysis via FTIR-ATR. Indeed, for both LCBF (Figs. 5A and SI13, Pragraph 2.7 of SI) and RMPF (Figs. 5B and SI14, Paragraph 2.8 in SI), it is evident that the degradation protocol ATM2.X induces a de-acetylation process characterized by an induction period of ca. 25 days as also observed for the data reported in Figs. 3 and 4. For both the supports, after 24 days of treatment, a decrease in the intensity of the peaks of the acetyl group (1220 and 1730 cm^{-1}) is observed together with the increase of the peak at 3330 cm^{-1} due to the increase of the polarity of the polymer and to the absorption of moisture.

4.3.4. Tensile tests

Finally, tensile tests were carried out on RMPF and Fig. SI15A and B (Paragraph 2.9 in SI) show the obtained results. The RMPF, as already observed for the exposure to HCl 5 M, were subjected to a decrease of the Young's Modulus (from 14.6 ± 0.9 MPa for P9_HCl5M to 7.3 ± 0.2 MPa for P48_ATM2.9). A very interesting finding was that when the RMPF had already been degraded by HCl 5 M, the re-starting of the degradation process produced an immediate decrease in Young's Modulus without any induction pe-

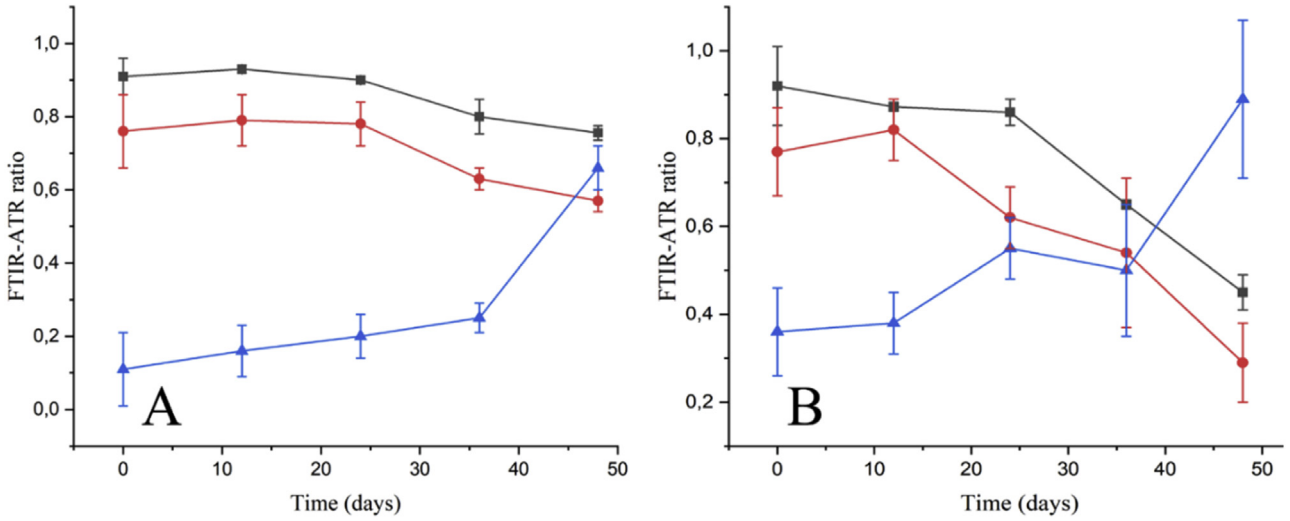

Fig. 5. FTIR-ATR ratios I_{1220}/I_{1030} (black), I_{1750}/I_{1030} (red) and I_{3330}/I_{1030} (blue) as a function of time during the third step of ATM2.X degradation protocol for LCBF (A) and RMPF (B). The results of each measurement are expressed as the average values and the corresponding standard deviations calculated from five spectra acquired in different areas of the film subjected to the same degradation protocol. The x-axis indicates the time of exposure to RH = 100% and room temperature after the previous two steps of the treatment.

riod, as observed in Fig. SI11B (Paragraph 2.6 in SI, P12_ATM2.9 shows a Young's Modulus of 9 ± 1 MPa). In addition, plastic deformation before 40 N is observed in all the samples after the third step of the ATM2.9 degradation protocol.

As indicated in Paragraph 4.2.4, even in this case, the TGA analysis (Fig. SI16 of Paragraph 2.9 in SI) indicates a decrease in the pyrolysis temperature with the increase of the degradation time. This effect could be attributed to the formed acetic acid and the residual HCl.

4.4. The validation of the multi-analytical method

To validate the multi-analytical method, the kinetics data describing the progress of the degradation process obtained through different analytical approaches through the procedures reported in the previous paragraphs (weight loss, acetyl content via HSM, free acidity and ATR-FTIR ratio), were normalised between 0 and 100 according to Eq. (5) and compared.

$$Normalised\ Value(\mathrm{NV}) = [(x - x_{min})/x_{max} - x_{min})] \times 100 \qquad (5)$$

Where x is the value of the investigated parameter at time t, x_{min} and x_{max} are the minimum and the maximum value of the parameter x respectively.

The normalised curves of the weight loss, correct acetyl content, ATR-FTIR ratios and free acidity data are reported in Fig. 6, for LCBF (Fig. 6A) and RMPF (Fig. 6B) subjected to the HCl 5 M degradation procedure. Data between weight loss, correct acetyl content, ATR-FTIR ratios and free acidity within a sample set are in appreciable agreement with each other: both the duration of the induction period of the de-acetylation process, equal to approximately 6 days for LCBF (Fig. 6A) and 9 days for RMPF (Fig. 6B), and the slope of the subsequent segment (6–16 days range for LCBF and 9–30 days range for RMPF) of the curves describing the trend of the weight loss, the correct acetyl content and the ATR-FTIR ratio were very similar for each class of samples (between - 8.2 and - 9.9 ca. for LCBF and between - 4.5 and - 5.6 for RMPF). Tables SI3 and SI4 (Paragraph 2.10 in SI) report all the linear regression parameters.

In Fig. 7 the NV curves of the weight loss, correct acetyl content, ATR-FTIR ratios, and free acidity data relative to LCBF and RMPF subjected to the ATM2.X protocol (to promote the re-starting and the evolution of the degradation process) were reported. The graphs in Fig. 7A show that the data for LCBF were in appreciable agreement with each other. Conversely, for RMPF (Fig. 7B), the normalized gravimetry data were not superimposable to the ones relative to acetyl content and the ATR-FTIR ratio. This behavior could be ascribed to the presence of the emulsion layer (that is not present in the LCBF) which, during the third step of the degradation protocol, may adsorb part of the environmental moisture (as also confirmed by the FTIR-ATR data, Fig. SI14 and Fig. 5B) or can be lost due to solubilization of the gelatine at high RH. Nevertheless, apart from this datum, the duration of the induction period of the de-acetylation process measured was around 24±12 days for both LCBF and RMPF. Furthermore, the slope of the subsequent segment (24–48 days) of all the curves is quite coherent and ranged between −3.4 (weight loss), −3.0 (correct acetyl content), −3.5 (ATR-FTIR ratio) and 3.0 (free acidity)-for LCBF and between - 2.1 (weight loss), - 3.7 (correct acetyl content), - 3.6 (ATR-FTIR ratio and 3.2 (free acidity) for RMPF (see Tables SI5 and SI6, Paragraph 2.10 in SI).

On these bases, it was possible to conclude that all the techniques used to monitor the evolution of the de-acetylation process of both LCBF and RMPF gave similar and coherent results.

Finally, in Fig. SI17 and Table SI7 (Paragraph 2.11 in SI) the trends of the correct acetyl content measured for both LCBF and RMPF subjected to the different degradation protocols were reported and commented for comparison. For all the protocols, it was possible to observe that the process was characterized by an initial "induction period" followed by a faster stage where the slope of the curve increased. Fig. SI17A and B show that the faster de-acetylation process was registered for LCBF samples subjected to the HCl 5 M degradation protocol, while the same protocol applied on RMPF induced a slower de-acetylation, as indicated by the slopes of the curves equal to - 3.5 (R^2 = 0.96) in the ranges 6–16 days and - 1.6, (R^2 = 0.99) in the range 9–30 days, for LCBF and RMPF, respectively (Table SI7). This difference was probably due to the presence of the emulsion layer, which acts as a stabilizer. Moreover, probably for the same reason, the induction period was longer for RMPF than for LCBF (9 days versus 6 days). Concerning the degradation protocols for the re-starting of the "vinegar syndrome" (ATM2.X), Fig. SI17C and D indicate that, in both these cases, the de-acetylation in LCBF and RMPF occurred at a lower rate than for LCBF and RMPF subjected to the HCl 5 M degradation protocol, because the exposure to the acid catalyst was limited to

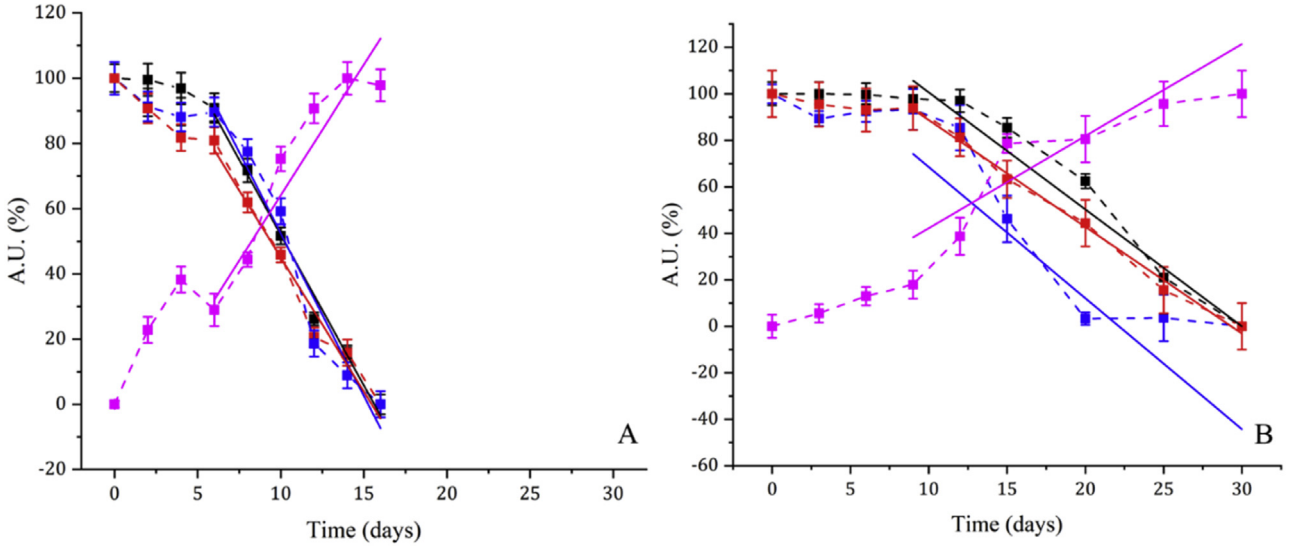

Fig. 6. Normalized values (Eq. 7) of weight loss (black), correct acetyl content (red), ATR-FTIR ratios (blue) and free acidity (magenta) data for (A) LCBF and (B) RMPF subjected to the HCl 5 M degradation protocol. The solid lines represent the best linear fitting of the segment of the curves after the induction time (6–16 days range for LCBF and 9–30 days range for RMPF). The fitting parameters are reported in Tables SI3 and SI4 (Paragraph 2.10 in SI).

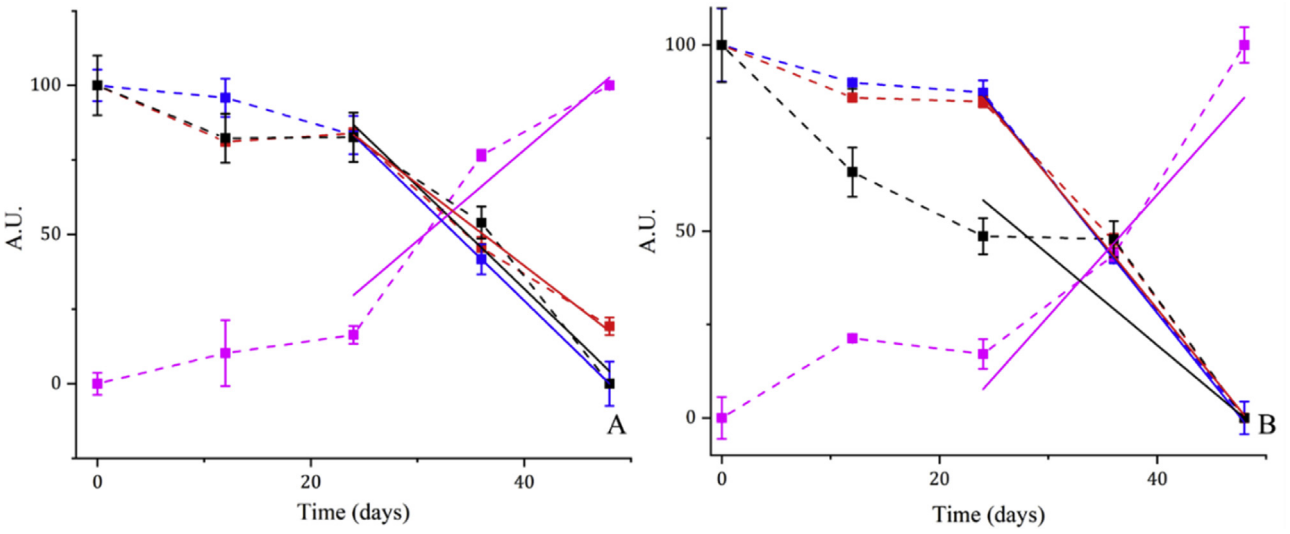

Fig. 7. NV (Eq. 7 weight loss (black), correct acetyl content (red), ATR-FTIR ratios (blue), and free acidity (magenta) data for (A) LCBF and (B) RMPF subjected respectively to the ATM2.3 and to the ATM2.9 degradation protocol. The x-axis indicates the time of exposure to RH = 100% and room temperature after the previous two steps of the treatment. The solid lines represent the best linear fitting of the segment of the curves after the induction time (24–48 days range for LCBF and RMPF). The fitting parameters are reported in Tables SI5 and SI6 (Paragraph 2.10 of SI).

the first step of the test. This was confirmed by the slope of the curves in the range 24–48, which, is −0.4 for LCBF and −0.3 for RMPF (Table. SI7).

5. Conclusions

A new way to artificially induce the “vinegar syndrome” to evaluate the performance of smart materials for the inhibition of this degradation phenomenon was set up. We succeeded in inducing the “vinegar syndrome” to a certain extent, stopping it, and re-starting it in a soft way to not damage the inhibitors that should be tested after the stop. The first step of the “vinegar syndrome” induction, which had to be strong enough to produce a consistent amount of acetic acid, was developed by submitting both the LCBF and the RMPF to an HCl-saturated atmosphere for a defined period. A consistent de-acetylation in both LBCF and RMPF was observed. After stopping the process, when the degradation reached a certain extent, the way of re-starting the “vinegar syndrome” was achieved by a two-step procedure: first, conditioning the samples to RH ca. 50% and room temperature for 24 h, and then curing the samples at room temperature and 100 % RH. Due to the very soft conditions (RH 100 % and room temperature) for triggering the re-starting and evolution of the degradation processes, no relevant physico-chemical alterations are expected on possible polymeric inhibitors subjected to this degradation protocol.

The multi-analytical method based on the calculation of the acetyl content through HSM (corrected with free acidity), of the ratios between the intensities of some ATR-FTIR diagnostic peaks seems to be a powerful and useful tool to follow the evolution of the artificially induced de-acetylation process that simulates the “vinegar syndrome” on both LCBF and RMPF. Indeed, comparing the linear fittings calculated on the normalised data, the equations of the curves that describe the correct acetyl content, the ATR-FTIR ratio, and the free acidity were coherent. The use of ATR-FTIR spec-

troscopy was considered a great alternative to HSM because it is a non-invasive and non-destructive technique that allows the collection of many spectra onto a film sample. Moreover, tensile tests gave precious information about collateral degradation pathways in RMPF which are promoted by de-acetylation (i.e. variation in the molecular weight of CA chains).

According to the above remarks, we can conclude that both the artificial induction of the "vinegar syndrome" and the multi-analytical protocol for its monitoring developed in the present study offer new bases for the evaluation of the performance of possible inhibitors of the "vinegar syndrome" in motion picture films, on time scale compatible with the laboratory timelines. The next step of our study will be the application of the results of the present paper on the evaluation of some inhibitors set up for preventing the "vinegar syndrome" in real motion picture films made of cellulose acetate.

Acknowledgments

The present study is a part of the PhD dissertation by Francesca Porpora entitled: "*Development of an innovative methodology for the treatment of cellulose triacetate motion picture films affected by the "vinegar syndrome"*. Financial support from University of Florence *Fondi d'Ateneo per la Ricerca* and *Fondi d'Ateneo per il Dottorato* are gratefully acknowledged. FP thanks *Ministero dell'Università e della Ricerca* (MUR) of Italy, Project PRIN 2022 2022XX8BRT PNRR, "*SMarT4BioArCH*", CUP Master B53DZ3014020006, financed by the European Union – Next Generation EU, for the Postdoc Fellowship. Thanks are due to the "*Istituto Agrario*" (*Technical Institute for Agronomy*), Florence, Italy for kindly providing the motion picture films.

Supplementary materials

Supplementary material associated with this article can be found, in the online version, at doi:10.1016/j.culher.2024.11.013.

References

[1] P. Read, M.P. Meyer, Restoration of Motion Picture Film, Butterwort, Oxford, 2000.
[2] M. Valverde, Photographic negatives: nature and evolution of processes, (2005) 9–18. http://www.bcin.ca/Interface/openbcin.cgi?submit=submit&Chinkey=235796.
[3] Y. Shashoua, Conservation of Plastics: Materials science, Degradation and Preservation, Elsevier Ltd, Oxford, 2008.
[4] M. McGath, S. Jordan-Mowery, M. Pollei, S. Heslip, J. Baty, Cellulose acetate lamination: a literature review and survey of paper-based collections in the United States, Restaurator 36 (2015) 333–365, doi:10.1515/res-2015-0015.
[5] É.C.T.C. Roldão, A contribution for the preservation of cellulose esters black and white negatives, Faculdade de Ciências e Tecnologia (FCT), Universidade Nova de Lisboa(PT), 2018.
[6] A.T. Ram, Archival preservation of photographic films–a perspective, Polym. Degrad. Stab. 29 (1990) 3–29, doi:10.1016/0141-3910(90)90019-4.
[7] K.A.H. Brems, The archival quality of film bases, SMPTE J. 97 (1988) 991–993.
[8] J.M. Reilly, Preserving photograph collections in research libraries: a perspective, Issues in the Conservation of Photographs, 1st ed., Getty Conservation Institute, Los Angeles, 2010.
[9] P.Z. Adelstein, J.M. Reilly, D.W. Nishimura, C.J. Erbland, Stability of cellulose ester base photographic film: Part I laboratory testing procedures, SMPTE J. (1992) 336–346.
[10] N.S. Allen, M. Edge, J.H. Appleyard, T.S. Jewitt, C.V. Horie, D. Francis, Degradation of historic cellulose triacetate cinematographic film: the vinegar syndrome, Polym. Degrad. Stab. 19 (1987) 379–387, doi:10.1016/0141-3910(87)90038-3.
[11] M. Edge, N.S. Allen, M. Hayes, P.N.K. Riley, C.V. Horie, J. Luc-Gardette, Mechanisms of deterioration in cellulose nitrate base archival cinematograph film, Eur. Polym. J. 26 (1990) 623–630, doi:10.1016/0014-3057(90)90218-S.
[12] M. Edge, N.S. Allen, T.S. Jewitt, J.H. Appleyard, C.V. Rorie, The deterioration characteristics of archival cellulose triacetate base cinematograph film, J. Photogr. Sci. 36 (1988) 199–203, doi:10.1080/00223638.1988.11737000.
[13] M. Edge, N.S. Allen, D.A.R. Williams, F. Thompson, V. Horie, Methods for predictive stability testing of archival polymers: a preliminary assessment of cellulose triacetate based motion picture film, Polym. Degrad. Stab. 35 (1992) 147–155, doi:10.1016/0141-3910(92)90106-F.
[14] P.Z. Adelstein, J.M. Reilly, D.W. Nishimura, C.J. Erbland, J.L. Bigourdan, Stability of cellulose ester base photographic film: Part V - recent findings, SMPTE J. 104 (1995) 439–447, doi:10.5594/J17707.
[15] M. Edge, N.S. Allen, T.S. Jewitt, C.V. Horie, Fundamental aspects of the degradation of cellulose triacetate base cinematograph film, Polym. Degrad. Stab. 25 (1989) 345–362, doi:10.1016/S0141-3910(89)81016-X.
[16] W. Lee, The stability film bases of Kodak professional motion-picture, in: Society of Motion Picture and Television Engineering, 1988, pp. 911–914.
[17] J.L. Bigourdan, Stability of acetate film base: accelerated-aging data revisited, J. Imaging Sci. Technol. 50 (2006) 494–501, doi:10.2352/J.ImagingSci.Technol.(2006)50:5(494).
[18] J.M. Reilly, IPI storage guide for acetate film, J. Am. Inst. Conserv. 33 (1994) 321, doi:10.2307/3179643.
[19] B. Knight, Lack of evidence for an autocatalytic point in the degradation of cellulose acetate, Polym. Degrad. Stab. 107 (2014) 219–222, doi:10.1016/j.polymdegradstab.2013.12.002.
[20] A. Al Mohtar, M.L. Pinto, A. Neves, S. Nunes, D. Zappi, G. Varani, A.M. Ramos, M.J. Melo, N. Wallaszkovits, J.I. Lahoz Rodrigo, K. Herlt, J. Lopes, Decision making based on hybrid modeling approach applied to cellulose acetate based historical films conservation, Sci. Rep. 11 (2021) 1–13, doi:10.1038/s41598-021-95373-0.
[21] D.M.W.M. Derham, M. Edge, D.A.R. Williams, The degradation of cellulose triacetate studied by nuclear magnetic resonance spectroscopy and molecular modelling, in: C.V.N.S. Allen, M. Edge, Horie (Eds.), Polymers in Conservation Conference, Royal Society of Chemistry, 1992.
[22] D. Littlejohn, R.A. Pethrick, A. Quye, J.M. Ballany, Investigation of the degradation of cellulose acetate museum artefacts, Polym. Degrad. Stab. 98 (2013) 416–424, doi:10.1016/j.polymdegradstab.2012.08.023.
[23] J. Ballany, D. Littlejohn, R.A. Pethrick, A. Quye, Probing the factors that control degradation in museum collections of cellulose acetate artefacts, ACS Symp. Ser. 779 (2001) 145–165, doi:10.1021/bk-2001-0779.ch012.
[24] P.Z. Adelstein, J.M. Reilly, D.W. Nishimura, C.J. Erbland, J.L. Bigourdan, Stability of cellulose ester base photographic film: Part V-recent findings, in: Studies of Incubation Techniques Long-Term Incubations of Polyester Base Film Properties of Naturally Aged Films on Acetate Base Infectious Behavior in Acetate Base Film, 1995, pp. 439–447.
[25] J. Bigourdan, J.M. Reilly, Effectiveness of storage conditions in controlling the vinegar syndrome: preservation strategies for acetate base motion-picture film collections, image and sound archiving and access: the challenges of the 3rd millenium, in: Proceedings of the Joint Technical Symposium, 2000, pp. 14–34.
[26] D. N, Strategies for the storage of cellulose acetate film, AIC News 40 (2015) 6–7.
[27] J.L. Bigourdan, P.Z. Adelstein, J.M. Reilly, Use of microenvironments for the preservation of cellulose triacetate photographic film, J. Imaging Sci. Technol. 42 (1998) 155–162.
[28] E. Kodak, Molecular sieve acid scavenger, (n.d.). https://www.kodak.com/en/motion/page/molecular-sieve-acid-scavenger.
[29] A.J. Cruz, J. Pires, A.P. Carvalho, M. Brotas de Carvalho, Comparison of adsorbent materials for acetic acid removal in showcases, J. Cult. Herit. 9 (2008) 244–252, doi:10.1016/j.culher.2008.03.001.
[30] A. João Cruz, J. Pires, A.P. Carvalho, M. Brotas de Carvalho, Adsorption of acetic acid by activated carbons, zeolites, and other adsorbent materials related with the preventive conservation of lead objects in museum showcases, J. Chem. Eng. Data 49 (2004) 725–731, doi:10.1021/je034273w.
[31] D. Yamamoto, T. Ishii, A. Hashimoto, K. Matsui, Use of sodium carbonate and sodium polyacrylate for the prevention of vinegar syndrome, Imaging Sci. J. 67 (2019) 171–178, doi:10.1080/13682199.2019.1577594.
[32] B. Lavédrine, A Guide to the Preventive Conservation of Photograph Collections, Getty Publ, Los Angeles, 2003.
[33] J.-L. Bigourdan, P.Z. Adelstein, J.M. Reilly, Effect of paper alkaline reserve on the chemical stability of acetate base sheet film, Top. Photogr. Preserv. 7 (2000) 43–54 http://resources.conservation-us.org/pmgtopics/1997-volume-seven/07_07_Bigourdan.pdf.
[34] K. Dedecker, R.S. Pillai, F. Nouar, N. Steunou, E. Dumas, G. Maurin, C. Serre, L. Pinto, Metal-Organic frameworks for cultural heritage preservation: the case of acetic acid removal, (2018). https://doi.org/10.1021/acsami.8b02930.
[35] A. Al Mohtar, M.I. Severino, P. Tignol, L. Ranza, A. Neves, F. Nouar, V. Pimenta, J. Lopes, A.M. Ramos, J.I.L. Rodrigo, M.J. Melo, N. Wallaszkovits, M.L. Pinto, A.-L. Dupont, C. Serre, B. Lavédrine, Iron(III) based metal-organic frameworks in cellulose acetate film preservation: fundamental aspects and first application, J. Cult. Herit. 66 (2024) 236–243, doi:10.1016/j.culher.2023.11.013.
[36] K. Dedecker, R. Pillai, F. Nouar, J. Pires, N. Steunou, E. Dumas, G. Maurin, C. Serre, M. Pinto, K. Dedecker, R. Pillai, F. Nouar, J. Pires, N. Steunou, Metal-Organic frameworks for cultural heritage preservation : the case of acetic acid removal to cite this version : HAL Id : hal-01791096(2021).
[37] Imaging materials - processed silver-gelatin type black-and white film - specifications for stability, 18901:2010(E), 2010.
[38] M.C. Fischer, J.M. Reilly, Use of passive monitors in film collections, AIC 6 (1995) 11–40.
[39] M.B. Harthan, J. C, M. Edge, N.S. Allen, The development and evaluation of a sensory system to detect degradation in cellulose triacetate photographic film. Part II: selection of a solid support for the indicator and field trials on indicator performance, Imaging Sci. J. 45 (1997) 81–83, doi:10.1080/13682199.1997.11736380.
[40] Standard test methods of testing cellulose acetate, D87–96, 2019.

[41] P.Z. Adelstein, J.M. Reilly, D.W. Nishimura, C.J. Erbland, Stability of cellulose ester base photographic film: Part III - measurement of film degradation, SMPTE J. 104 (1995) 281–291.
[42] K. Curran, M. Strlič, Polymers and volatiles: using VOC analysis for the conservation of plastic and rubber objects, Studi. Conserv. 60 (2015) 1–14, doi:10.1179/2047058413Y.0000000125.
[43] K. Curran, M. Underhill, L.T. Gibson, M. Strlic, The development of a SPME-GC/MS method for the analysis of VOC emissions from historic plastic and rubber materials, Microchem. J. 124 (2016) 909–918, doi:10.1016/j.microc.2015.08.027.
[44] K. Curran, A. Možir, M. Underhill, L.T. Gibson, T. Fearn, M. Strlič, Cross-infection effect of polymers of historic and heritage significance on the degradation of a cellulose reference test material, Polym. Degrad. Stab. 107 (2014) 294–306, doi:10.1016/j.polymdegradstab.2013.12.019.
[45] R. Casarano, L.C. Fidale, C.M. Lucheti, T. Heinze, O.A. El, Expedient, accurate methods for the determination of the degree of substitution of cellulose carboxylic esters : application of UV – vis spectroscopy (dye solvatochromism) and FTIR, Carbohydr. Polym. 83 (2011) 1285–1292, doi:10.1016/j.carbpol.2010.09.035.
[46] S. Nunes, F. Ramacciotti, A. Neves, E.M. Angelin, A.M. Ramos, É. Roldão, N. Wallaszkovits, A.A. Armijo, M.J. Melo, A diagnostic tool for assessing the conservation condition of cellulose nitrate and acetate in heritage collections : quantifying the degree of substitution by infrared spectroscopy, Herit. Sci. (2020) 1–14, doi:10.1186/s40494-020-00373-4.
[47] S. Da Ros, A.E. Aliev, I. del Gaudio, R. King, A. Pokorska, M. Kearney, K. Curran, Characterising plasticised cellulose acetate-based historic artefacts by NMR spectroscopy: a new approach for quantifying the degree of substitution and diethyl phthalate contents, Polym. Degrad. Stab. 183 (2021) 109420, doi:10.1016/J.POLYMDEGRADSTAB.2020.109420.
[48] H. Kono, H. Hashimoto, Y. Shimizu, NMR characterization of cellulose acetate : chemical shift assignments, substituent effects, and chemical shift additivity, Carbohydr. Polym. 118 (2015) 91–100, doi:10.1016/j.carbpol.2014.11.004.
[49] P. Fei, L. Liao, B. Cheng, J. Song, Quantitative analysis of cellulose acetate with a high degree of substitution by FTIR and its application, Anal. Methods 9 (2017) 6194–6201, doi:10.1039/c7ay02165h.
[50] N.S. Allen, M. Edge, J.H. Appleyard, T.S. Jewitt, C.V. Horie, D. Francis, Acid-catalysed degradation of historic cellulose triacetate, cinematographic film: influence of various film parameters, Eur. Polym. J. 24 (1988) 707–712, doi:10.1016/0014-3057(88)90002-X.
[51] N.S. Allen, M. Edge, T.S. Jewitt, C.V. Horie, Initiation of the degradation of cellulose triacetate base motion picture film, J. Photogr. Sci. 38 (1989) 54–59, doi:10.1080/00223638.1989.11737073.
[52] T. Heinze, T. Liebert, Celluloses and Polyoses/Hemicelluloses, Elsevier B.V., 2012, doi:10.1016/B978-0-444-53349-4.00255-7.
[53] U. Siemann, Solvent cast technology - a versatile tool for thin film production, Prog. Colloid. Polym. Sci. 130 (2005) 1–14, doi:10.1007/b107336.
[54] Y. Yamashita, T. Endo, Deterioration behavior of cellulose acetate films in acidic or basic aqueous solutions, J. Appl. Polym. Sci. 91 (2004) 3354–3361, doi:10.1002/app.13547.
[55] M.L. Nelson, Relation of certain infrared bands to cellulose crystallinity and crystal lattice type. Part 11. A new infrared ratio for estimation of crystallinity in celluloses I and II*, J. Appl. Polym. Sci. 8 (1964) 1325–1341.
[56] E. Carretti, M. Milano, L. Dei, P. Baglioni, Noninvasive physicochemical characterization of two 19th century English ferrotypes, J. Cult. Herit. 10 (2009) 501–508, doi:10.1016/j.culher.2009.02.002.
[57] Image Permanence Institute (IPI)., No Title, (n.d.). https://filmcare.org/index.
[58] Z. Jia, Y. Li, Y. Qi, Y. Zhou, D. Hu, X. Chao, H. Xing, J. Li, Study on microbubble of cellulose acetate microfilm of the Republic of China (AD 1912–1949) collected in the Second Historical Archives of China, Herit. Sci. 8 (2020) 1–10, doi:10.1186/s40494-020-00374-3.
[59] M.R. Huang, X.G. Li, Thermal degradation of cellulose and cellulose esters, J. Appl. Polym. Sci. 68 (1998) 293–304, doi:10.1002/(SICI)1097-4628(19980411)68:2⟨293::AID-APP11⟩3.0.CO;2-Z.